Blast Hazard Resilience Using Machine Learning for West Fertilizer Plant Explosion

Zhenhua Huang, A.M.ASCE[1]; Liping Cai[2]; and Tejaswi Kollipara[3]

Abstract: To investigate the effect of infrastructure traits on resilience after an exploration, a blast case (West Fertilizer Plant in West, Texas, 2013) was studied, in which all the buildings' damage data (damage pictures, damage scales, and building locations) and resilience information (recovery decision, recovery time, and recovery cost) were collected by authors through site visits, interviews, and appraisal data collections. The novel analysis methods and machine learning algorithms (logistical/linear regression, neural networks, k-nearest neighbor, support vector machine, and gradient boosting) were applied to analyze the West Fertilizer Plant explosion resilience. This study is unique because it implements a resilience analysis for an explosion hazard, although there are some reports discussing the resilience after natural hazards, such as earthquakes, tsunamis, hurricanes, and tornados. Additionally, using machine learning for resilience analysis is also unique. The results can assist decision-makers, civil engineers, and building designers in designing the most resilient structures and/or materials for buildings. The findings in this study can help to develop the most resilient buildings, communities, and cities by considering the impact of explosion hazards. **DOI: 10.1061/(ASCE)CF.1943-5509.0001644.** *© 2021 American Society of Civil Engineers.*

Author keywords: Explosion resilience; Explosion; Recovery decision; Recovery cost; Machine learning modeling.

Introduction

Accidents in the past have revealed that explosions would have serious consequences for personnel, buildings, communities, society, and environments, as well as economic systems. There were many studies discussing explosion hazard risks. Risk is the possibility of something bad happening in the future, which could be dangerous or have a bad result. There is a strong need for studies to investigate the explosion hazard resilience, which expresses recovery capacities in infrastructures, social and economic systems, and environments after disasters.

West Fertilizer Plant Explosion and Explosion Hazard Risks

At the West Fertilizer Plant in West, Texas, an ammonium nitrate explosion occurred on April 17, 2013. More than 150 buildings were damaged or destroyed. This explosion caused approximately $100 million in damages to homes, businesses, and schools near the fertilizer plant (Reuters 2013). After the explosion, the damage severities of 76 damaged buildings among the 150 practically damaged buildings were examined by the authors (Huang et al. 2016). There were some studies discussing the West Fertilizer Plant Explosion to date in which the cause of the explosion and the government regulations were mostly discussed. Yonekawa et al. (2014) proposed some improvements for safety suggestions. Jennings and Matthiessen (2015) reported that the West explosion triggered efforts by the federal government to improve their coordination with local governments and federal agencies to update policies, regulations, and standards and pay attention to safe work practices. Laboureur et al. (2016) identified gaps between the West explosion and current regulations and then recommended emergency response procedures and provided suggestions for modifying the current regulations to prevent or minimize future losses. Babrauskas (2016, 2017) and Davis et al. (2017) pointed out that untrained fertilizer mill personnel caused this ammonium nitrate (AN) explosion. The explosions of the AN fertilizer in storage caused uncontrollable fires, suggesting the implementation of fertilizer formulations to reduce uncontrolled fire possibilities and adopt building safety measures against uncontrolled fires. Han et al. (2016, 2017) indicated that the safer use of AN fertilizers is needed to be reinforced. Huang et al. (2020) carried out the blast risk assessment of wood residential buildings for the West explosion case.

There were some studies that discuss explosion hazard risks. For example, Gorev and Medvedev (2017) investigated the parameters of the blast wave passing through a screen placed in its path. It was found that the degree of pressure reduction behind the barrier depended on its permeability, the relative size of the obstacles, the length of the positive phase of the wave, and the degree of removal of waves from the source. It was concluded that such obstacles could serve as effective explosion protection. Russo et al. (2019) reported that the failure of high-pressure hydrogen gas pipelines and subsequent explosion might induce heavy damage to buildings. Damage to both types of structural components was evaluated, and the maximum distance of blast damage was derived in several environmental conditions, contributing to land-use planning and performance-based design/assessment of pipelines and buildings. After an explosion, the remaining capacity of a structure to resist a progressive collapse was analyzed by Eskew and Jang (2020), which can provide information for emergency operations and decision-makers. A method to estimate the remaining elemental structural capacity of a postblast structure involved using the alternate path method to assess an updated numerical model, which incorporated the buildings' structural damage. The proposed

[1]Associate Professor, Dept. of Mechanical Engineering, Univ. of North Texas, Denton, TX 76207 (corresponding author). ORCID: https://orcid.org/0000-0001-5990-8425. Email: zhenhua.huang@unt.edu

[2]Researcher, Dept. of Mechanical Engineering, Univ. of North Texas, Denton, TX 76207. Email: liping.cai@unt.edu

[3]Research Assistant, Dept. of Mechanical Engineering, Univ. of North Texas, Denton, TX 76207. Email: tejaswikollipara@my.unt.edu

Note. This manuscript was submitted on February 8, 2021; approved on June 8, 2021; published online on August 2, 2021. Discussion period open until January 2, 2022; separate discussions must be submitted for individual papers. This paper is part of the ***Journal of Performance of Constructed Facilities***, © ASCE, ISSN 0887-3828.

method can be used to assess a structure's potential for progressive collapse after a blast, leading to safer emergency operations. Song et al. (2021) developed a quantitative risk assessment methodology for gas leakage and explosion accident consequences inside residential buildings, as well as proposed effective risk reduction measures.

The preceding explosion hazard literature review revealed that most studies about explosion hazards discussed the risks and causes of the explosion-induced damages and relevant government regulations; no report regarding the resilience of explosion hazards and the application of machine learning in explosion hazards has been found by the authors. There is a strong need for such studies. Therefore, after a few years of the West explosion, the recovery information of damaged buildings was collected and documented by the authors through revisiting the explosion site, examining the rebuilt/repaired buildings, talking with the local government and residents, and searching building appraisals. The 76 damaged buildings, including 67 residential buildings, 5 medical buildings (such as nursing homes and clinic office buildings), and 4 educational buildings (e.g., schools), were utilized to develop resilience models using machine learning techniques in this study.

Resilience Analysis

Driven by the increased multihazard exposure and consequences worldwide, hazard resilience has received arising interest in research. Hazard resilience describes adaptive capacities in infrastructures, social/economic systems, and environments after disasters (Jonkeren et al. 2014; Kumaraswamy et al. 2015).

Recently, resilience has become the forefront topic; however, implementation of resilience research in practice remains challenging. Bergstrand et al. (2015) measured municipal resilience and social vulnerability in counties across the US and found a correlation between high vulnerability and low resilience. It was revealed that counties in the West were most vulnerable while counties in the Southeast were prone to low resilience. By considering both social vulnerability and municipal resilience, it can map social risks for attacks from hazards as well as their capacities for recovering from the hazard aftermath. This finding can assist in emergency planning and response, as well as be tailored toward reducing damages or resilience from multihazards. Modica and Zoboli (2016) evaluated socioeconomic losses after natural disasters using the developed relationships among hazard, risk, damage, vulnerability, and resilience, which can be used as a guideline for the assessment of the socioeconomy.

Opdyke et al. (2017) reviewed 241 scientific papers from 1990 to 2015 for investigating resilience research trends, analysis methods, and recovery variables, as well as correlations between each of these categories. Most published reports were carried out using qualitative methods, focusing on infrastructure and community units of analysis, and examining governance, infrastructure, and economic dimensions. It was recommended that future work should conduct deeper quantitative resilient investigations with mixed methods to analyze infrastructure and community connectedly and to measure environmental and social dimensions of resilience quantitively. Liu et al. (2018) evaluated the county resilience of moderate earthquakes with magnitudes ranging from 5.0 to 7.0 based on 102 moderate earthquakes that occurred during 2002–2014. The results suggested that most counties in China exhibited low efficiency and resilience capability after being attacked by moderate earthquakes. Using the Tobit regression model, the insurance intensity, hospital beds, government financial expenditure, and disaster experience were analyzed, and strategies to improve county resilience were proposed.

Masoomi et al. (2018) investigated the risk and community resilience of the wood-frame residential buildings under hurricanes and tornados. It proposed methods for improving the wind performance of roof coverings, roof sheathing nailing patterns, and roof-to-wall connection types for wood-frame residential buildings. The damage fragilities of the wood-frame building archetypes were considered for four damage scales defined based on the performance of the building envelope, including roof coverings, doors and windows, roof sheathing, and roof-to-wall connections. Then, it is also compared with the existing method amplifying wind pressures in the wind standards to represent a tornado load. The fragility curves provided in the study can be used to represent residential buildings within a community for risk or resilience assessment/mitigation under hurricane or tornado loadings.

Capozzo et al. (2019) combined fragility functions of earthquake intensity and tsunami inundation with regional hazard data to estimate damages and economic losses of civil infrastructure for the coastal city of Seaside, Oregon. It was found that the loss estimation was tremendously increased when the earthquake and tsunami were considered together. Dhulipala and Flint (2020) modeled the resilience of civil infrastructure systems after being attacked by multiple hazards using a semi-Markov model. The function recovery of these systems was estimated by considering the interevent dependencies. The model was developed by considering many aspects, such as a three-state system exposed to random occurrences of identical hazard events and multihazard resilience of a building considering seismic and wind hazards.

The relationship between building attributes and tornado vulnerability was developed using a Logistic regression model (Egnew et al. 2018). The building attributes included the year built, location, appraised cost, and stories. The effect of wind speed and building attributes on the observed damage scales to residential buildings was quantified using the multinomial logistic regression model. It was found that newer homes and homes with a lower value per unit living area increased the likelihood of tornado damages. The number of stories weakly correlated with the increasing likelihood of higher levels of tornado damage. The information on earthquake-induced building damages after an earthquake was collected using multisource remote sensing images (Li et al. 2019). The feature analysis was conducted based on the Rough set theory. A logistic regression model was used to establish the relationship between the occurrence and absence of destroyed buildings within an individual object. The comparison with the survey results proved that the detection accuracy of the proposed method was 94.2%. This approach illustrated that multivariate logistic regression could be used to compare different features for applications in the field of damage detection.

Although the hazard resilience of infrastructures has been placed high on the priority list of development of infrastructures, there remain challenges in implementing resilience in practice. This study proposed a novel explosion hazard resilience analysis method to evaluate the resilience level in practice quantitively. Through the literature review, it was discovered that some reports were discussing resilience research after natural hazards, such as earthquakes, tsunamis, hurricanes, and tornados. However, no report about the resilience after explosion hazards was found by the authors. And no study using advanced machine learning algorithms for the resilience analysis, such as the artificial neural network (ANN), k-nearest neighbor (kNN), support vector machine (SVM), and gradient boosting, was found by the authors.

This study conducted explosion hazard resilience analysis using machine learning algorithms, which is novel because it implemented a resilience analysis for explosion hazards. The resilience analysis for explosion hazards is as important as that for natural

hazards. Natural hazards are considered recurrently happening and cannot be controlled easily. Explosion hazards should be considered similarly because similar explosions happened regularly and recurrently at similar communities, although maybe not at the exact same location. According to the data in the Annual Explosives Incident Report of the US (USBDC 2019), the explosion incidents in the US were 912 in 2014, 630 in 2015, 699 in 2016, 687 in 2017, and 706 in 2018, which were caused similarly by ammonium nitrate, binary explosives, black powder, black powder substitutes, chlorate/perchlorate mixtures, dry ice, flash powder/pyrotechnic mixture, improvised/homemade explosives (HME)–fuel oxidizer mixture, hexamethylene triperoxide diamine (HMTD), hydrogen peroxide mixtures, ignitable gas, ignitable liquid, and others. The total number of explosion incidents is much higher than that of an earthquake or tsunami in the US. The annual number of explosion incidents from 2014 to 2018 indicated that, like natural hazards, similar explosion hazards cannot be controlled easily and happened recurrently in similar communities, while maybe not in the exact same community. Therefore, there is a need to explore the resilience analysis for explosion hazards.

Another novelty of this study was that the analysis methods of machine learning algorithms (ANN, kNN, SVM, and gradient boosting) were applied to analyze the practical resilience after an explosion hazard. A relationship between the resilience variables (recovery decision, recovery time, and recovery cost) and nine input predictor variables (building category, building structure, wall surface material, roof surface material, building stories, blocked or not, distance from the blast center, year built, and shockwave overpressure) was established. As a result, it was reported that the importance level of the individual predictor variable contributed to each target variable. It is known that the social cost of strictly controlling the risk in one or a few factories in a certain area could be smaller than the cost for improving resistance to protect all-around buildings from explosions; however, a resilience model can provide a deeper understanding and more information on the resilience than just social cost, such as if an explosion hazard already happened and how long and how much should be expected for the recovery of the community. Therefore, it is worth the time and effort to conduct a resilience analysis for explosion hazards. The findings of this research will help government decision-makers, architects, civil engineers, and building designers choose the most resilient structure design and/or materials for residential and commercial buildings, as well as plan the most resilient buildings, towns, and cities by taking explosion hazards into account.

Predictive Models Using Machine Learning Techniques

The flowchart of the predictive modeling of blast hazard resilience is presented in Fig. 1. The data of the West Fertilizer Plant explosion damaged buildings, and their repair/rebuild information was imported into the Machine Learning program as shown in the first step (file import node) in Fig. 1. The input and target variables were defined in this step. Four target variables (damage scale, recovery decision, recovery time, and recovery cost) and nine input variables (building category, building structure, wall surface material, roof

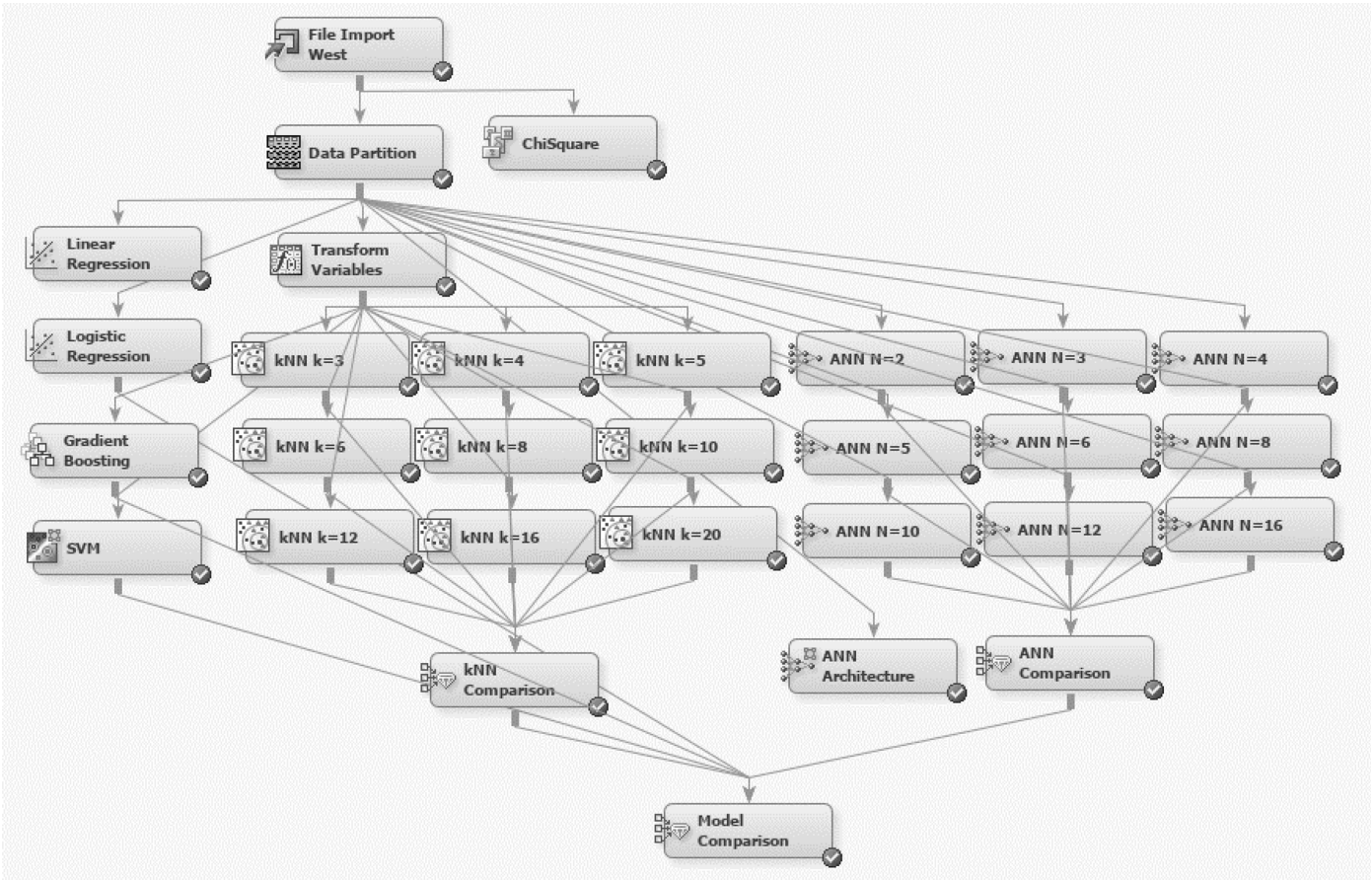

Fig. 1. Flowchart of predictive models of explosion hazard resilience.

J. Perform. Constr. Facil., 2021, 35(5): 04021062

Table 1. Description of input variables

No.	Variables	Abbreviation	Variable description
1	Building category	BC	Residential, educational, and medical
2	Building structure	—	Masonry, steel, and wood
3	Wall surface material	S_{wall}	Brick, brick/hardiprank, brick/metal, hardiplank, and stucco
4	Roof surface material	—	Asphalt shingles or metal
5	Building stories	—	One or two stories
6	Blocked or not	B	Unblocked or blocked
7	Distance from blast center	D	The damaged house to blast center (m)
8	Year built	Y	The year the house was built
9	Shockwave overpressure	P_s	The shockwave overpressure in kPa

surface material, building stories, blocked or not, distance from blast center, year built, and shockwave overpressure) were selected, as listed in Table 1. A detailed description of these input and target variables and the logic for the variable selection are described in the "Input and Target Variables" section. Following the file import node, the Chi-Square test (StatExplore Chi node) was used to examine the relative relationship between the target variable and each independent input variable. The data partition node in Fig. 1 randomly sorted the imported data into the training group (70%) and the validation group (30%). After the data sorting, machine learning nodes, including logistic regression, linear regression, k-nearest neighbor, support vector machines, artificial neural networks, and gradient boosting were performed (Fig. 1). Finally, these results of modeling and validation were compared, and the optimal strategy that can make the lowest damage scale was achieved.

Chi-Square for Comparison of Variable Importance

A Chi-square test is used to examine the importance of an individual independent variable among many variables for contributing the target variable and to test the fitness of the observed data distribution with the expected distribution. Categorical variables can be analyzed successfully by a Chi-square test (Ahmadi et al. 2016). Numerical variables can be sorted into several bins and treated as categorical variables for the Chi-square test. Chi-square (χ^2) can be calculated by squaring differences between the observed and expected data frequencies, being divided by the expected frequency to normalize values, and then summed as shown in Eq. (1)

$$\chi^2 = \sum_{i=1}^{n} \frac{(O_i - E_i)^2}{E_i} \tag{1}$$

where O_i = observed data frequency; and E_i = expected data frequency. For example, for the block or not variable, the observed data frequencies are 22 and 54 (Fig. 2), and the expected data frequency is 38, which is the average of 22 and 54.

Logistic and Linear Regression Analysis

Because some target variables in this study (e.g., damage scale and recovery decision) are not continuous, the traditional linear regression models' response variable output is not appropriate in this study due to the nominal nature of classifiers. Therefore, a multinomial logistic regression model is used for nominal responses (Egnew et al. 2018). Although logistic regression is similar to linear regression, it is required to use the *logit link function* for solving the problem of the nonnormal distribution of categorical target variables. A link function is simply a function of the mean of the target variable Y that is used as the target instead of Y itself. All that means is when Y is categorical, the logit of Y is used as the target in a regression equation instead of just Y (Parzen et al. 2011). The logit function is the natural log of the odds that Y equals one of the categories. If P is a probability, then $P/(1-P)$ is the corresponding odds; the *logit* of the probability is the logarithm of the odds as Eq. (2)

$$\ln\left(\frac{P(Y \le j)}{1 - P(Y \le j)}\right) = \ln\left(\frac{\pi_1 + \cdots + \pi_j}{\pi_{j+1} + \cdots + \pi_J}\right) = \alpha_j + \beta_1 X_1 + \cdots + \beta_p X_p \tag{2}$$

where Y = target category; j = index of the categories from $1, \ldots, J-1$, with J being the total number of categories; π = probability of a given target category; α = intercept of the model; and β = effect of predictor X on the log odds of the target in category j or below. For J categories, there are $J-1$ equations, with the values of β constant for each equation but with differing intercepts, α.

Automatic selections of multiple variables [X in Eq. (2)] have three of the most common methods, which are backward elimination, forward selection, and stepwise selection (Austin and Tu 2004). In the backward elimination process (adopted in this study), by beginning with a full model consisting of all candidate predictor variables, variables are sequentially eliminated from the model until a prespecified stopping rule is satisfied. At a given step of the elimination process, the variable whose elimination would result in the smallest decrease in a summary measure is eliminated. Possible summary measures are deviance or R^2. The most common stopping rule is that all variables that remain in the model are significant at a prespecified significance level.

As one of the most popular and simplest techniques for machine learning predictive modeling, a multiple linear regression analysis, is used to build a relationship between the numerical target and input variables using a mathematical algorithm as follows (Tso and Yau 2007)

$$y = \beta_0 + \beta_1 x_1 + \beta_2 x_2 + \cdots + \beta_p x_p + \varepsilon \tag{3}$$

where y = target variable; β_i = regression coefficient ($I = 0, 1, 2, \ldots, p$); x_i = input predictor variables ($i = 1, 2, \ldots, p$); and ε = random error term.

In machine learning modeling, using the linear regression analysis, the relationship between output target variables and input known as features and numeric value categorized as predictors can be mapped (Gujar and Vakharia 2019).

k-Nearest Neighbor

The essential theory of the k-nearest neighbor is a process for finding a group of k samples that are nearest to unknown samples based on distance functions in the calibration dataset (Noi and Kappas 2018). From these k samples, the labels (class) of unknown samples are

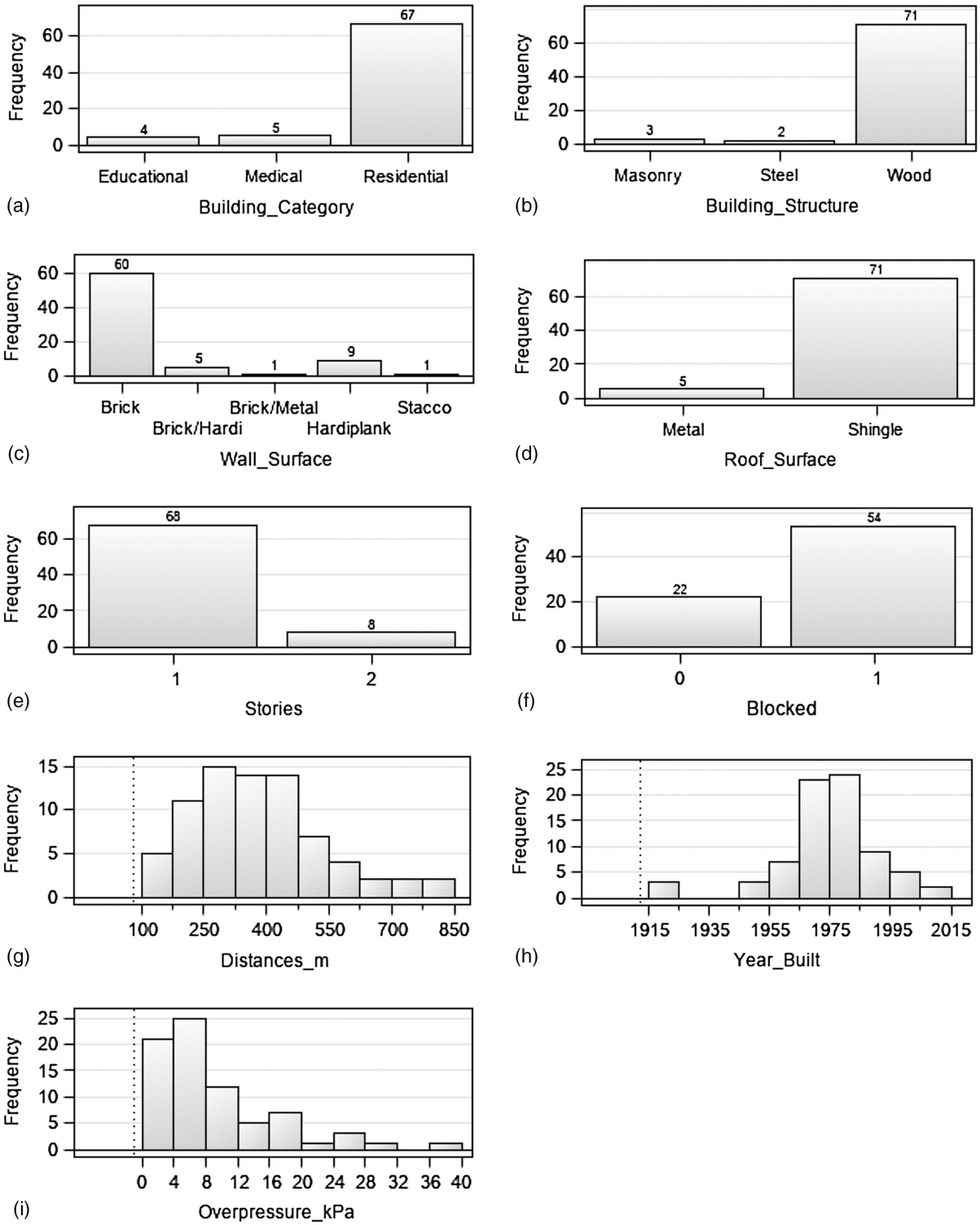

Fig. 2. Distributions of nine input variables: (a) building category; (b) building structure; (c) wall surface material; (d) roof surface material; (e) building stories; (f) blocked or not; (g) distance from blast center; (h) year built; and (i) shockwave overpressure.

determined by calculating the average of the response variables, namely, the class attributes of the k nearest neighbor. As a result, for this classifier, the k plays an important role in the performance of the kNN, which is the key tuning parameter of kNN. Using a bootstrap procedure, the parameter k was estimated. In this study, k values were examined from 1 to 20 to identify the optimal k value for all training sample sets.

Support Vector Machine

The support vector machine can handle nonseparable data, which generalizes the optimal separating hyperplane as the solution to minimize a cost function that expresses a combination of two criteria: margin maximization and error minimization to penalize the wrongly classified samples (Melgani and Bruzzone 2004). The cost function can be expressed as follows

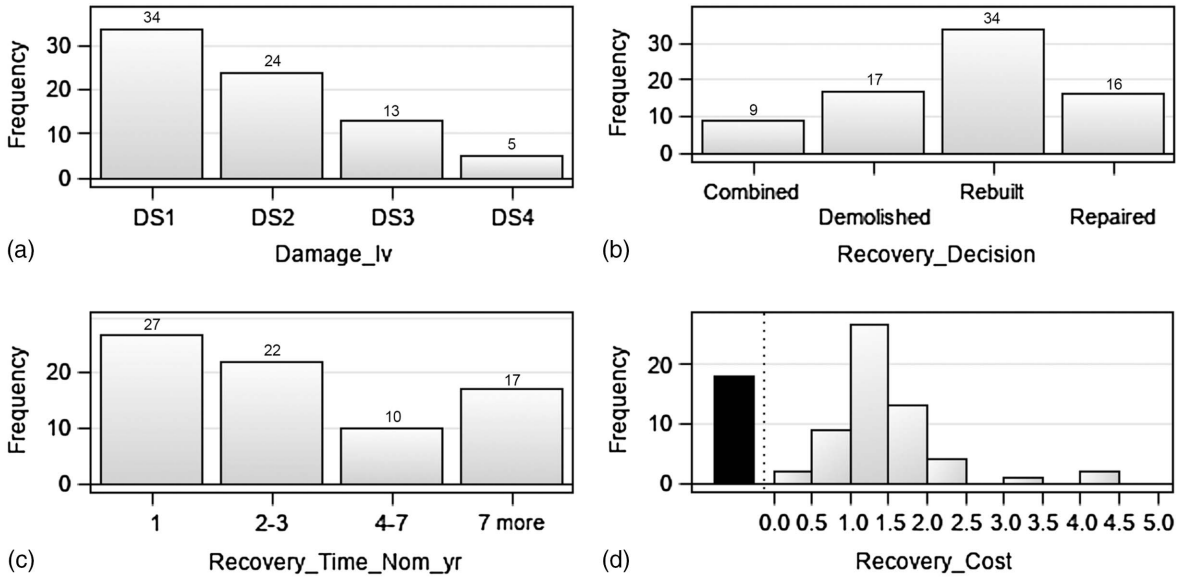

Fig. 3. Distributions of four target variables: (a) damage level; (b) recovery decision; (c) recovery time; and (d) recovery cost.

$$\Psi(w,\xi) = \frac{1}{2}\left\|w\right\|^2 + C\sum_{w}^{n}\xi_i \tag{4}$$

where ξ_i = slack variables to account for the nonseparability of data; and the constant C = regularization parameter that allows controlling the penalty assigned to errors. The larger the C value, the higher the penalty to misclassified samples. The minimization of the cost function described in Eq. (4) is subject to the constraints of Eq. (5)

$$y_{i(w\cdot x_i+b)\geq 1-\xi_i,} \quad i=1,2,\ldots,N \tag{5}$$

$$\xi_i \geq 0, \quad i = 1, 2, \ldots, N$$

Artificial Neural Network

The artificial neural network is one of the advanced machine learning algorithms based on the model of a human neuron, which works like the way the human brain processes information. As one of the most well-known and widely adopted machine learning methods, the ANN model enables learning from a training dataset and stores the pattern of the data simulating connections of neurons (Kumar et al. 2011). After training, when new data is applied to the ANN algorithm, it recognizes the pattern from the data and classifies it. Finally, the algorithm gives results quickly and accurately. Fig. 4 shows a typical multilayer ANN structure. The ANN models consist of three layers: input, hidden, and output. The input layer represents the input variables, while the output layer shows target variables. The hidden layer, where the data are processed, is presented between the input and output layers. Moreover, the hidden layer is essential for nonlinear data. Each layer includes an array of artificial neurons. Therefore, each of the neurons is connected with the succeeding or proceeding layers. This research adopts a multilayer perceptron (MLP) architecture of the ANNs with a weighted linear combination function [Eq. (6)] and the hyperbolic tangent activation function [Eq. (7)]. The most popular back-propagation optimization method was adopted

$$H_j = \sum_{i=1}^{n}(w_{ij}x_i) + b_j \tag{6}$$

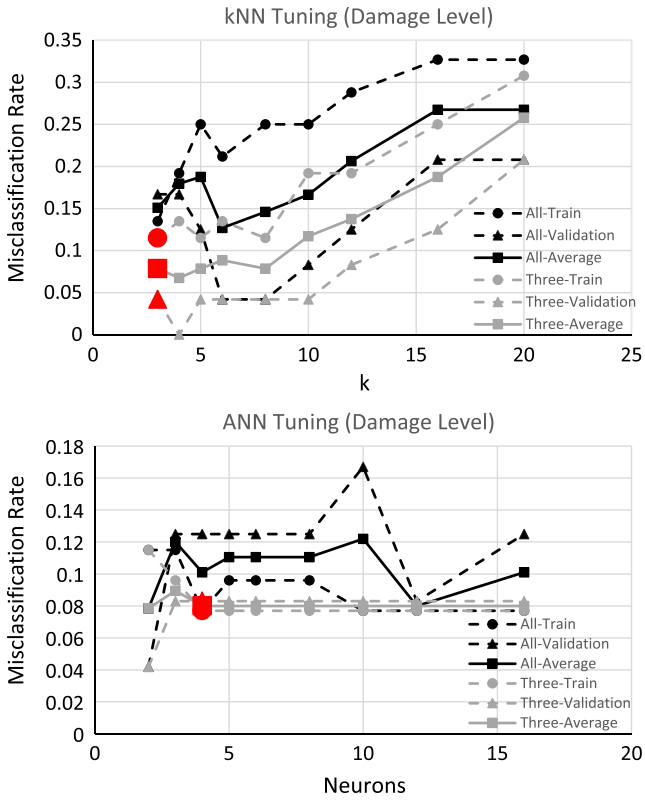

Fig. 4. Tuning of k-nearest neighbor and artificial neural network for damage scale.

$$y_j = \tanh(\beta H_j) \tag{7}$$

where x_i = input of a neuron; b = bias; w_i = weight coefficient; β = constant coefficient; and y = output of the neuron.

The number of inputs and number of hidden neurons of the ANN models in this study were selected using the trial and error method with the best misclassification rate (categorical target

J. Perform. Constr. Facil., 2021, 35(5): 04021062

Table 2. Description of target variables

No.	Variables	Abbreviation (unit)	Variable description
1	Damage scale	DS	Minor damage (DS1), moderate damage (DS2), severe damage (DS3), and destruction (DS4)
2	Recovery decision	D_{recovery}	Demolished, rebuilt, repaired, and combined
3	Recovery time	t_{recovery}	Recovery time in years (years)
4	Recovery cost	C_{recovery}	The ratio of the appraisal price of the building after recovery and before the house damage.

variable) or smallest root mean squared errors (numerical target variable). The trial models include the following: (1) with all variables, (2) with significant variables based on Chi-square analysis, and (3) with significant variables based on regression analysis. During the calculation, 70% of the total data was used for the training process, and 30% of data was used for the validation process in this study.

Gradient Boosting

As one subtechnique of decision trees, gradient boosting models are a sequential assembly of different decision trees. According to several subtrees, prediction makes these models more robust. Gradient boosting involves three key elements as follows: a loss function to be optimized, a weak learner (decision tree) used to make predictions, and an additive model for adding weak learners to minimize the loss function. The high complexity of gradient boosting models provides the models with good prediction power, which makes the models very useful for variable selections. However, the interpretability of the models is reduced because of the high complexity (Yuan 2015).

Input and Target Variables

Input Variables

In this study, the input predictor variables and their descriptions are listed in Table 1. Among these nine variables, six of them (building category, building structure, wall surface material, roof surface material, building stories, and year built) were selected according to the FEMA published natural hazard analysis tool HAZUS version 4.2 (FEMA 2011); the other three (distance from the blast center, shockwave overpressure, and blocked or not) were selected according to the explosion hazard risk analysis by Huang et al. (2016).

A total of 76 damaged buildings onsite of the explosion was documented and discussed in this study, including 67 residential buildings, 5 medical buildings (such as a nursing home or clinic office building), and four educational buildings (e.g., schools), as shown in Fig. 2(a). Among the 76 buildings, there were 71 wooden structures, 3 masonry structures, and 2 steel structures [Fig. 2(b)]; as for the building surface materials, there were 60 buildings with a brick wall surface, 9 buildings with hardiplank, 5 with brick/hardiplank, 1 with brick/metal, and 1 with stucco, as shown in Fig. 2(c); as for roof surface material, there were 71 buildings with asphalt shingles and 5 with metal [Fig. 2(d)]; as for building stories, there were 68 single-story buildings and 8 two-story buildings [Fig. 2(e)]; there were 22 unblocked buildings and 54 blocked buildings, as shown in Fig. 2(f); the distribution of distance from the blast center ranged from 100 to 900 m as shown in Fig. 2(g); the year of the house built ranged from 1915 to 2015, as shown in Fig. 2(h); and the distribution of shockwave overpressure ranged from 0 to 40 kPa, as shown in Fig. 2(i).

Target Variables

In this study, there were four target variables, as listed in Table 2, describing damage and resilience information, including the (1) damage scale, (2) recovery decision, (3) recovery time, and (4) recovery cost, as shown in Table 2 and Fig. 3. The damage scales (DS) (Huang et al. 2016) were set as a target categorical variable, in which four damage levels were sorted. For example, for the wood residential buildings, the four levels are described as the following: minor damage (DS1), showing typical window glass breakage, large and small windows shattered, occasional damage to window frames, and minor damage to house surfaces; moderate damage (DS2), showing moderate roof damage (i.e., small deflections, large size, or amount of shingle torn-offs), moderate brick façade damage (i.e., small areas of collapse and cracks), and moderate wall panels damage (i.e., small holes on the wood panel, metal panel failure, and buckling); severe damage (DS3), showing severe roof surface damage (i.e., holes and large deflections), severe wall surface damage (i.e., a large area of façade collapse and large holes on wood panels), and some structural member damage; and destruction (DS4), showing the collapse of roofs and walls and failures of structural members. See the study by Huang et al. (2016) for a detailed description of the DS for other types of buildings. Among the 76 buildings, 34 of them could be categorized in DS1 (minor damage), 24 in DS2 (moderate damage), 13 in DS3 (severe damage), and 5 in DS4 (destruction), as shown in Fig. 3(a).

In this study, the resilience information of the explosion-damaged buildings (the three resilience target variables: recovery decision, recovery time, and recovery cost) was collected by authors through site visits, interviews, and online appraisal data collections. As for the recovery decision, there were 17 demolished buildings, 34 rebuilt buildings, 15 repaired buildings, and 9 combined buildings (i.e., someone bought a neighbor's yard and built a larger building), as shown in Fig. 3(b). As for recovery time, there were 27 buildings rebuilt within 1 year, 22 buildings rebuilt in 2–3 years, 10 rebuilt in 4–7 years, and 17 still not rebuilt yet after 7 years, as shown in Fig. 3(c). As for recovery cost, which is the ratio of the appraisal price of the building after recovery and before the building damage, there were 2 buildings' cost ratios ≤ 0.5, 9 buildings' cost ratio ranging from 0.5 to 1, 27 buildings' ratios ranging from 1 to 1.5, 13 buildings' ratios ranging from 1.5 to 2, 7 buildings' ratios higher than 2, and 18 damaged buildings still being not repaired or not rebuilt (0 repairment/rebuild cost), as shown in Fig. 3(d).

Because this study had four target variables, i.e., damage scale, recovery decision, recovery time, and recovery cost, the machine learning models were performed four times to achieve four optimal machine learning models. The Stage 1 analysis sets the damage scale as the target variable and the nine predictor variables (Table 1) as inputs. The Stage 2 analysis sets the recovery decision as the target variable and the nine predictor variables (Table 1) plus the damage scale as inputs. The Stage 3 analysis sets the recovery time as the target variable and the nine predictor variables (Table 1) plus the damage scale and recovery decision as inputs. The Stage 4 analysis sets the recovery cost as the target variable and the nine

predictor variables (Table 1) plus the damage scale, recovery decision, and recovery time as inputs.

Results and Discussions

Damage Scale

When the damage scale was set as a target variable, the inputs were nine independent variables, i.e., building category, building structure, wall surface material, roof surface material, building stories, blocked or not, distance from the blast center, year built, and shockwave overpressure.

Firstly, a Chi-square analysis was carried out to explore the importance of the nine input variables. The results of the Chi-square analysis are presented in Table 3. In Table 3, the Chi-square (χ^2) is the calculated values according to Eq. (1), Df is the degrees of freedom, which is related to the numbers of categories of the categorical variables analyzed, Prob (P-value) is the probability of observing a sample statistic as extreme as the test statistic, and significant indicates which input variables significantly affect the target variable of the damage scale. The results indicated that, among the nine variables, three variables, i.e., shockwave overpressure ($P < 0.0001$), distance from the blast center ($P < 0.0001$), and blocked or not ($P = 0.0010$), significantly affected the building damage scale, as shown in Table 3.

Because the target variable of the building damage scale was sorted into four levels, which is not a continuous variable, the linear regression model is not appropriate in this study due to the nominal nature of classifiers (Egnew et al. 2018). Thus, a multinomial logistic regression model is used to predict the building damage scale. After inputting the nine independent variables into the logistic regression model, the output results were summarized and are listed in Table 4. Table 4 shows that the predictor variable of the shockwave overpressure was the only significant variable contributing to the damage scale ($P = 0.0003 < 0.05$ for DS3 and $P = 0.0037 < 0.05$ for DS2). For DS4, it is not significant because of the small amount of DS4 data (only five DS4 damages in the dataset).

Based on the results in Table 4, three logistic regression equations are presented as follows

$$\log(\text{Odds}_{DS4/DS1}) = -152.2 + 8.0719 \times P_{so} \quad (8)$$

$$\log(\text{Odds}_{DS3/DS1}) = -18.6643 + 2.5998 \times P_{so} \quad (9)$$

$$\log(\text{Odds}_{DS2/DS1}) = -10.7914 + 1.9131 \times P_{so} \quad (10)$$

where Odds_{DSi} = odds of two damage scales; and P_{so} = shockwave overpressure at the building location (m). Eqs. (8)–(10) depict that the higher the blast load, the higher probability of the higher damage scale is expected. This finding is consistent with the previous report by Huang et al. (2020). The set of equations has McFadden's pseudo R^2 of 0.762. The P-value for the Chi-square of the log-likelihood is smaller than 0.0001, which indicated good performance.

In addition to the regression model, the kNN, ANN, and gradient boosting machine learning models were created for the damage scale. Misclassification rates were used in this study to tune and compare different machine learning models for categorical target variables. When the selection of property is not suitable for classification, misclassification occurs. When all classes or categories of a variable have the same error rate or probability of being misclassified, it can be defined as misclassification.

Based on the description in the "k-Nearest Neighbor" section, kNN models were created with the standardized input variables with all input variables and the three significant input variables (shockwave overpressure, distance, and blocked), respectively. Fig. 4 presents the tuning procedure to optimize the k value based on the misclassification rate, which shows that when $k = 3$, the model provided a low average misclassification rate with a low variation.

Based on the method discussed in the "Artificial Neural Network" section, ANN models were created using the MLP architecture and backpropagation optimization with all input variables and the three significant input variables (shockwave overpressure, distance, and blocked), respectively. Based on the tuning procedure shown in Fig. 4, an ANN model with the three significant input variables and four hidden layer neurons in Fig. 5 were selected,

Table 3. Chi-square test results for damage scale s

Input	Chi-square	Df	Prob	Significant
Overpressure_kPa	129.0837	12	<0.0001	Yes
Distances_m	79.9185	12	<0.0001	Yes
Blocked	16.1982	3	0.0010	Yes
Year_built	13. 9963	12	0.3009	—
Wall_surface	12.4740	12	0.4084	—
Building_structure	5.5445	6	0.4761	—
Roof_surface	2.6635	3	0.4465	—
Building_category	2.4496	6	0.8741	—
Stories	0.7652	3	0.8578	—

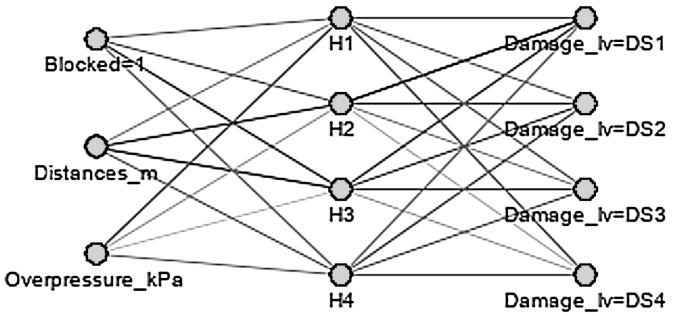

Fig. 5. ANN architecture for damage level.

Table 4. Results of logistic regression for damage scale as the target variable

Parameter	Damage_lv	Df	Estimate	Standard error	Wald Chi-square	Pr > ChiSq	Significant
Intercept	DS4	1	−152.2	1,569.3	0.01	0.9228	—
Intercept	DS3	1	−18.6643	4.8269	14.95	0.0001	Yes
Intercept	DS2	1	−10.7914	3.6920	8.54	0.0035	Yes
Overpressure_kPa	DS4	1	8.0719	64.2179	0.02	0.9000	—
Overpressure_kPa	DS3	1	2.5998	0.7239	12.90	0.0003	Yes
Overpressure_kPa	DS2	1	1.9131	0.6585	8.44	0.0037	Yes

Table 5. Comparison of misclassification rates between logistic regression and ANN models for damage scale as the target variable

Model	Train data	Validation data	Model bias	Model variation
Logistic regression	0.077	0.083	0.080	0.006
kNN $k = 3$	0.115	0.042	0.079	0.073
ANN $n = 4$	0.077	0.083	0.080	0.006
Gradient boosting $i = 60$	0.058	0.083	0.070	0.025

which provided a low average misclassification rate with low variation.

Based on the description in the "Gradient Boosting" section, a gradient boosting model was created with the maximum iterations (number of trees) equal to 200, the learning rate (shrinkage) equal to 0.1, and the maximum branch and depth of each tree equal to 2 and 2.

The comparison of misclassification rates among the logistic regression, kNN, ANN, and gradient boosting models for the damage scale as the target variable is shown in Table 5. It is illustrated that the biases of different models were low (0.07–0.08) and close to each other, which are acceptable. The gradient boosting model performed the best among the four models, which has the lowest model bias. However, the gradient boosting model varied more than the regression and ANN models.

Recovery Decision

When the recovery decision was set as a target variable, the inputs were 10 independent variables, i.e., damage scale, building category, building structure, wall surface material, roof surface material, building stories, blocked or not, distance from blast center, year built, and shockwave overpressure.

The target variable recovery decision had four selections (values), namely, demolished, rebuilt, repaired, or combined (with a neighbor's yard). The results of the Chi-square analysis are presented in Table 6. The results indicated that, among the 10 predictor variables, 3 variables, i.e., distance from the blast center ($P = 0.0022 < 0.05$), wall surface material ($P = 0.0067 < 0.05$), and damage scale ($P = 0.0053 < 0.05$) significantly affected the recovery decision, as shown in Table 6. Besides, the predictor variable of the year built had a P value of $0.0726 < 0.1$, which can also be considered a significantly contributed variable to the recovery decision (Table 6).

However, when the test of the misclassification rates was applied to examine the misclassification rates for the machine learning models, it was found that none of them was a reliable model. For example, the misclassification rates of the logistic regression model were larger than 40% for both training and validation data groups, while the misclassification rates of the ANN model were 22% for the training group and 34.6% for the validation group. Therefore, the recovery decision variable was redefined as a binary variable for further analysis.

Table 6. Chi-square analysis results for recovery decision as the target variable

Input	Chi-square	Df	Prob	Significant
Distances_m	30.7073	12	0.0022	Yes
Wall_surface	27.4244	12	0.0067	Yes
Damage_sc	23.4347	9	0.0053	Yes
Year_built	19.7175	12	0.0726	—
Overpressure_kPa	18.1125	12	0.1123	—
Stories	5.7752	3	0.1231	—
Blocked	3.6288	3	0.3044	—
Building_structure	5.2734	6	0.5093	—
Building_category	2.6396	6	0.8525	—
Roof_surface	0.9287	3	0.8185	—

Table 7. Chi-square analysis results for recovery decision as a binary target variable

Input	Chi-square	Df	Prob	Significant
Distances_m	25.2383	4	<0.0001	Yes
Damage_sc	19.8002	3	0.0002	Yes
Wall_surface	13.8278	4	0.0079	Yes
Overpressure_kPa	12.5050	4	0.0140	Yes
Year_built	7.6885	4	0.1037	—
Building_structure	1.4272	2	0.4899	—
Blocked	1.0246	1	0.3114	—
Stories	0.3935	1	0.5305	—
Building_category	0.0418	2	0.9793	—
Roof_surface	0.0036	1	0.9524	—

According to the test results of misclassification rates, the target variable recovery decision with four variables cannot produce effective models to predict the recovery decision. Thus, the recovery decision variable was redefined as a binary variable, which had two values only, i.e., C1 = repaired and C2 = reconstructed, including rebuilt, demolished, and combined.

The results of the Chi-square analysis are presented in Table 7. The results indicated that, among the 10 predictor variables, four variables, i.e., distance from the blast center ($P < 0.0001$), damage scale ($P = 0.0002 < 0.05$), wall surface material ($P = 0.0079 < 0.05$), and shockwave overpressure ($P = 0.0140 < 0.05$), significantly affected the recovery decision, as shown in Table 7.

Because the target variable of the recovery decision was defined as a binary target variable (C1 = repaired or C2 = reconstructed), which were not numerical variables, the linear regression model cannot be utilized. Thus, a multinomial logistic regression model was used to predict the recovery decision. After inputting 10 predictor variables into the logistic regression model, the output results were summarized and are listed in Table 8. Table 8 shows that the predictor variable of distance from the blast center was the only significant variable contributing to the recovery decision ($P = 0.0032 < 0.05$).

Based on the results in Table 8, a logistic regression equation was obtained and are presented as follows

$$\log\left(\frac{P_{C2}}{P_{C1}}\right) = 7.791 - 0.0153 \times D \tag{11}$$

where P_{Ci} = probability of the recovery decision (C1 = repaired or C2 = reconstructed); and D = distance from the blast center in meters. The equation has McFadden's pseudo R^2 of 0.384. The P-value for the Chi-square of log-likelihood is smaller than 0.0001, which indicated good performance. However, Eq. (11) only works for the condition of an explosion with a 15,000–20,000 kg equivalent TNT. For a more general explosion, the following equation could be used

$$\log\left(\frac{P_{C2}}{P_{C1}}\right) = -2.4495 + 0.7578 \times P_s \tag{12}$$

where P_s = shockwave overpressure in kPa. Eqs. (11) and (12) depict that, when the building was closer to the blast center and/or the blast load was higher, the probability of reconstructions instead of repairs was higher. This finding is consistent with common sense.

Table 8. Logistic regression modeling results for recovery decision as a binary target variable

Parameter	Recovery_decision_binary	Df	Estimate	Standard error	Chi-square	Pr > ChiSq	Significant
Intercept	C2	1	7.791	2.343	11.06	0.0009	Yes
Distances_m	C2	1	−0.0153	0.00521	8.69	0.0032	Yes

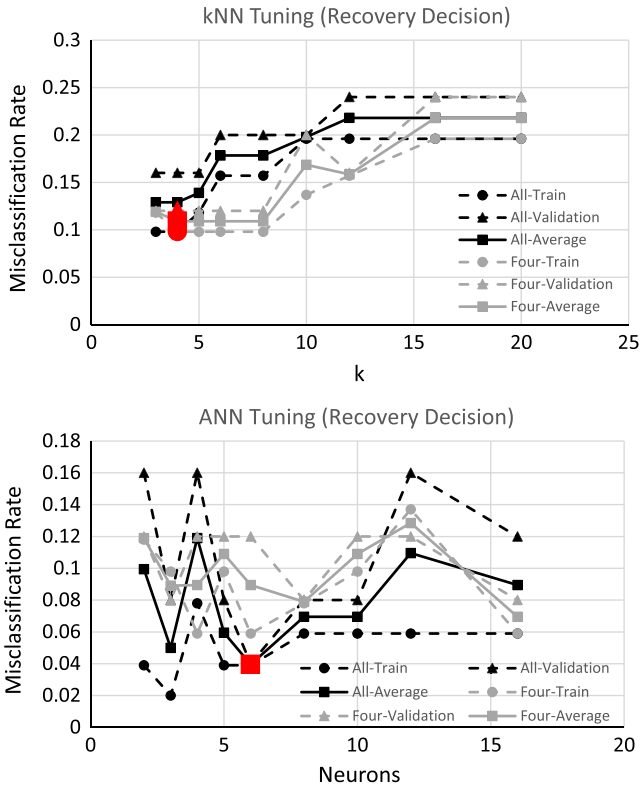

Fig. 6. Tuning of k-nearest neighbor and artificial neural network for recovery decision.

Similar to the models discussed in the "Damage Scale" section, the kNN, ANN, and gradient boosting models for predicting the recovery decision were created and tuned, as shown in Fig. 6. A kNN model with $k = 4$ and four significant input variables (shockwave overpressure, distance, damage level, and wall surface), an ANN model with 6 hidden layer neurons and all input variables (as shown in Fig. 7), and a gradient boosting model with iteration = 150 were selected. In addition, an SVM model was created based on the "Support Vector Machine" section. The comparison of misclassification rates among the five machine learning models for the recovery decision is shown in Table 9. Table 9 shows that all models' biases were acceptable (4%–11%). The ANN and gradient boosting models provided better prediction accuracy compared to other models. However, the gradient boosting model varies more than the ANN model.

Recovery Time

When recovery time was set as a target variable, the inputs were 11 predictor variables, i.e., recovery decision, damage scale, building category, building structure, wall surface material, roof surface material, building stories, blocked or not, distance from the blast center, year built, and shockwave overpressure.

The results of the Chi-square analysis are presented in Table 10. The results indicated that, among the 11 predictor variables, 2 variables, i.e., recovery decision ($P < 0.0001$) and blocked or not ($P = 0.0175 < 0.05$), significantly affected the recovery time, as shown in Table 10.

As a type of statistical process, a multivariate linear regression model can be used to construct a relationship between the predictor and target variables when the target variable is a numerical value. As for regression analysis, the relationship between the input known as features and the numeric value categorized as a predictor can be mapped (Gujar and Vakharia 2019).

In this study, the relationship between the 11 input variables and the target variable (recovery time) was developed, and the results are presented in Table 11. Table 11 presents the coefficients of variables significantly contributing to the target variable ($P < 0.05$), plus intercept, in the developed regression equation. As shown in Table 11, three variables (blocked or not, damage scale, and

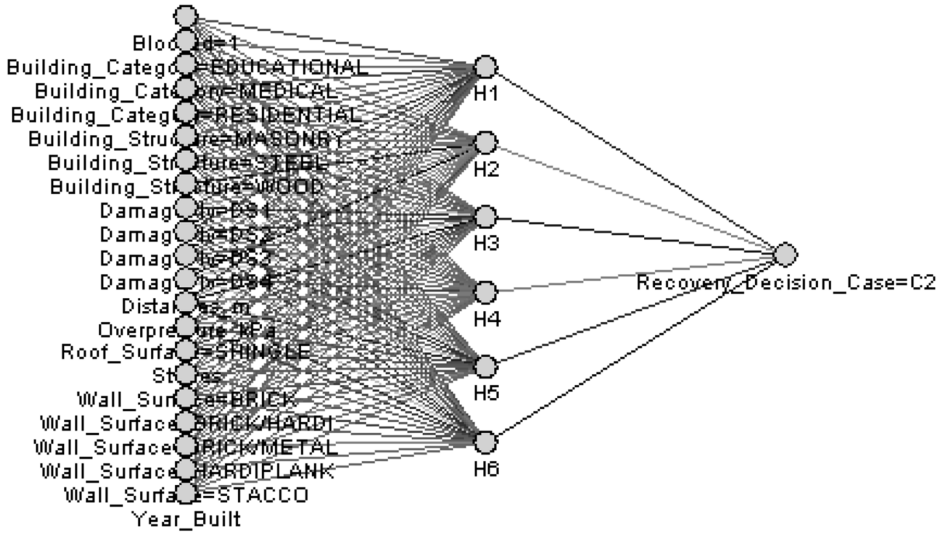

Fig. 7. ANN architecture for recovery decision.

Table 9. Comparison of misclassification rates between logistic regression and ANN models for recovery decision as a binary target variable

Model	Train data	Validation data	Model bias	Model variation
Logistic regression	0.098	0.12	0.109	0.022
kNN $k = 4$	0.098	0.12	0.109	0.022
SVM	0.098	0.12	0.109	0.022
ANN $n = 6$	0.039	0.04	0.040	0.001
Gradient boosting $i = 150$	0.000	0.08	0.040	0.080

Table 10. Chi-square analysis results for recovery time as the target variable

Input	Chi-square	Df	Prob	Significant
Recovery_decision	82.946	9	<0.0001	Yes
Blocked	10.1305	3	0.0175	Yes
Distances_m	17.519	12	0.1311	—
Year_built	15.9772	12	0.1923	—
Wall_surface	15.5592	12	0.2123	—
Overpressure_kPa	12.0001	12	0.4457	—
Roof_surface	2.8637	3	0.4131	—
Building_category	5.4695	6	0.4851	—
Stories	2.705	3	0.4394	—
Damage_sc	7.3688	9	0.5988	—
Building_structure	4.2511	6	0.6427	—

overpressure) out of 11 input variables significantly affected the target variable (recovery time).

The multivariate linear regression result for the recovery time as the target variable is presented as Eq. (13)

$$t_{\text{recovery}} = 3.3301 - 1.5916DS + 0.2327P_s + \text{B} \qquad (13)$$

$$R^2 = 0.3717, \quad Adj\,R^2 = 0.3221, \quad F = 7.49,$$
$$P\text{-value} = 0.0005$$

where t_{recovery} = recovery time in years; DS = damage scale from DS = 1 to DS = 4; Ps = shockwave overpressure in kPa; and B = block coefficient, which is equal to 0.6074 for the unblocked case and 0 for the blocked case. Based on Eq. (13), the following observations can be obtained: (1) the damage scale negatively affected the recovery time, indicating that the higher damage scale could result in a sooner rebuild or repair; (2) the higher shockwave overpressure made the longer recovery time; and (3) the block protection for a building can lower the recovery time. All the preceding observations are consistent with common sense.

Based on the descriptions in the "Support Vector Machine," "Artificial Neural Network," and "Gradient Boosting" sections, the kNN, ANN, gradient boosting models for predicting the recovery time were created and tuned, as shown in Fig. 8. The kNN model with $k = 3$ and three significant input variables (shockwave overpressure, damage level, and blocked), the ANN model with three

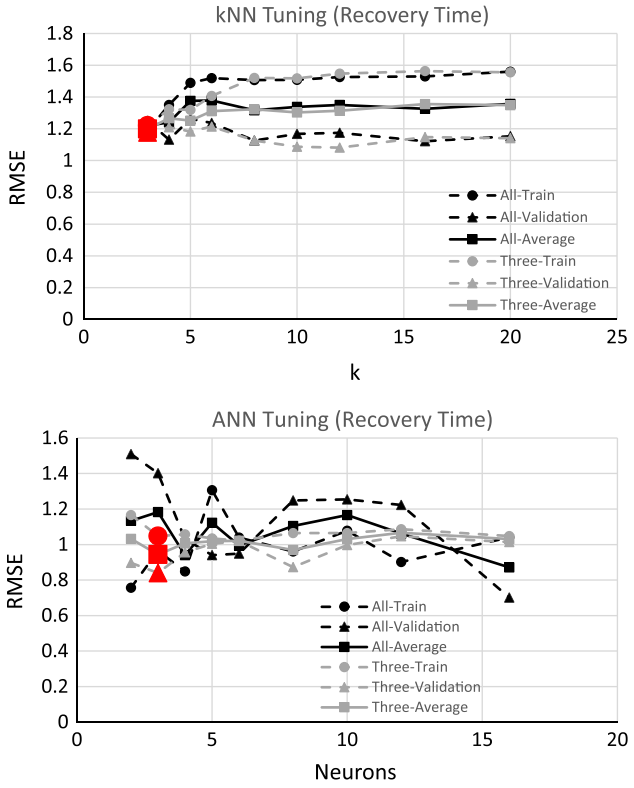

Fig. 8. Tuning of k-nearest neighbor and artificial neural network for recovery time.

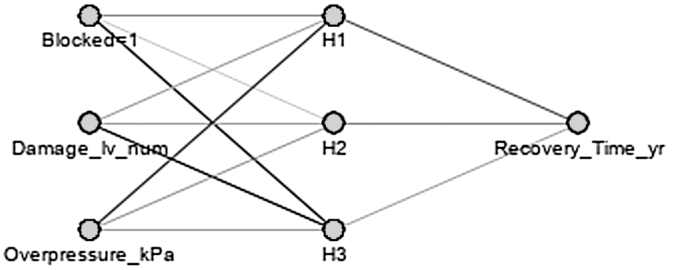

Fig. 9. ANN architecture for recovery time.

hidden layer neurons and three significant input variables (as shown in Fig. 9), and the gradient boosting model with iteration = 200 were selected.

The comparison of the root mean squared errors (RMSE) between the results of the linear regression and machine learning models for the recovery time as the target variable is listed in Table 12, which includes training data, validation data, averages, and variations. The RMSE [Eq. (14)] assumed that the model errors of n samples are calculated as (e_i, $i = 1, 2, \ldots, n$), which does not

Table 11. Multivariate linear regression modeling results for recovery time as the target variable

Parameter	Category	DF	Estimate	Error	t value	Pr $>\|t\|$	Significant
Intercept	—	1	3.3301	0.6712	4.96	<0.0001	Yes
Blocked	0	1	0.6074	0.2691	2.26	0.0298	Yes
Damage_sc_num	—	1	−1.5916	0.6448	−2.47	0.0182	Yes
Overpressure_kPa	—	1	0.2327	0.0793	2.93	0.0057	Yes

Table 12. Comparison of RMSEs between regression and machine learning models for recovery time

Model	Train data	Validation data	Model bias	Model variation
Linear regression	1.2861	0.8443	1.0652	0.4418
kNN $k = 3$	1.2193	1.1771	1.198	0.0422
ANN $n = 3$	1.0474	0.8399	0.944	0.2075
Gradient boosting $i = 200$	0.3456	1.1507	0.74815	0.8051

Table 13. Chi-square analysis results for recovery cost as the target variable

Input	Chi-square	Df	Prob	Significant
Recovery_time_nom_yr	93.1191	15	<0.0001	Yes
Recovery_decision	86.3217	15	<0.0001	Yes
Wall_surface	50.4708	20	0.0002	Yes
Building_category	18.6858	10	0.0444	Yes
Blocked	7.3657	5	0.1948	—
Year_built	25.8707	20	0.1701	—
Distances_m	24.9563	20	0.2031	—
Damage_lv	18.6737	15	0.2289	—
Overpressure_kPa	21.8187	20	0.3504	—
Stories	3.055	5	0.6915	—

consider the uncertainties brought in by observation errors or the method used to compare modeling and observation results (Chai and Draxler 2014). Besides, it is assumed that the error sample set is unbiased. The RMSE is described

$$\text{RMSE} = \sqrt{\frac{1}{n}\sum_{i=1}^{n} e_i^2} \tag{14}$$

The comparison of RMSE among the four machine learning models for the recovery time is shown in Table 12. Table 12 shows that all models' biases are acceptable (0.75–1.20 years). The gradient boosting model had the best prediction accuracy among the four models. However, the gradient boosting model varied more than other models.

Recovery Cost

When recovery cost was set as a target variable, the inputs were 12 independent variables, i.e., recovery time, recovery decision, damage scale, building category, building structure, wall surface material, roof surface material, building stories, blocked or not, distance from blast center, year built, and shockwave overpressure.

A Chi-square analysis was used to analyze the impact of 12 input variables on the target variable (recovery cost). The results of the Chi-square analysis are presented in Table 13. The results indicated that, among the 12 predictor variables, four variables, i.e., recovery time ($P < 0.0001$), recovery decision ($P < 0.0001$), wall surface material ($P = 0.0002 < 0.05$), and building category ($P = 0.0444 < 0.05$) significantly affected recovery cost, as shown in Table 13.

The linear relationship between 12 input variables and the target variable (recovery cost) was developed, and the results are presented as Eq. (15). Table 14 presents the coefficients of variables significantly contributing to the target variable ($P < 0.05$), plus intercept, in the developed regression equation. As shown in Table 14, four variables, i.e., building category (medical: $P = 0.0038$), recovery decision (C1 = repair: $P = 0.0391$), recovery time ($P = 0.0171$), wall surface material (brick: $P = 0.0012$, brick/hardi: $P < 0.0001$, brick/metal: $P = 0.0104$, and hardiplank: $P = 0.0118$), out of 12 input variables significantly affected the target variable (recovery cost).

The developed multivariate linear regression equation is given as Eq. (15)

$$C_{\text{recovery}} = 1.1014 + BC + D_{\text{recery}} + 0.1196t_{\text{recovery}} + S_{\text{wall}} \tag{15}$$

$$R^2 = 0.6140, \quad \text{and adjusted } R^2 = 0.5204,$$
$$F = 6.56, \quad P\text{-value} < 0.0001$$

where C_{recovery} = recovery cost, which is the ratio of the appraisal price of the building after recovery to the price before damage; BC = building category coefficient, which is 0 for residential, 0.0873 for educational, and 0.8801 for medical; D_{recovery} = recovery decision, which is −0.2141 for repair and 0 for reconstruction; t_{recovery} = recovery time in years; and S_{wall} = coefficient of wall surface material, which is 0.7133 for brick walls, 1.2584 for brick walls with hardiplank, −1.3678 for brick walls with metal plates, and 0.9124 for hardiplank walls. Based on Eq. (15), the following findings were observed: (1) building category affected recovery cost, indicating that the medical buildings needed the highest recovery costs, educational buildings needed medium costs, and residential buildings needed lowest costs; (2) recovery decision affected recovery cost, in which, reconstruction needed higher costs than repair; (3) recovery time positively affected recovery cost: the longer the time, the more expensive; and (4) wall surface material affected recovery cost, in which the cost was ranked from high to low in the following order: brick walls with hardiplank > hardiplank walls > brick walls > stucco > brick walls with metal plates.

Based on the description in the "Support Vector Machine," "Artificial Neural Network," and "Gradient Boosting" sections, the kNN, ANN, and gradient boosting models for predicting the recovery cost were created and tuned, as shown in Fig. 10.

Table 14. Multivariate linear regression analysis results for recovery cost as the target variable

Parameter	Category	DF	Estimate	Error	t value	Pr $>\|t\|$	Significant
Intercept	—	1	1.1014	0.2001	5.5	<0.0001	Yes
Building_category	Educational	1	0.0873	0.3442	0.25	0.8014	—
Building_category	Medical	1	0.8801	0.2822	3.12	0.0038	Yes
Recovery_decision	C1	1	−0.2141	0.0997	−2.15	0.0391	Yes
Recovery_time_yr	—	1	0.1196	0.0476	2.51	0.0171	Yes
Wall_surface	Brick	1	0.7133	0.2004	3.56	0.0012	Yes
Wall_surface	Brick/hardi	1	1.2584	0.2763	4.55	<0.0001	Yes
Wall_surface	Brick/metal	1	−1.3678	0.5036	−2.72	0.0104	Yes
Wall_surface	Hardiplank	1	0.9124	0.3424	2.66	0.0118	Yes

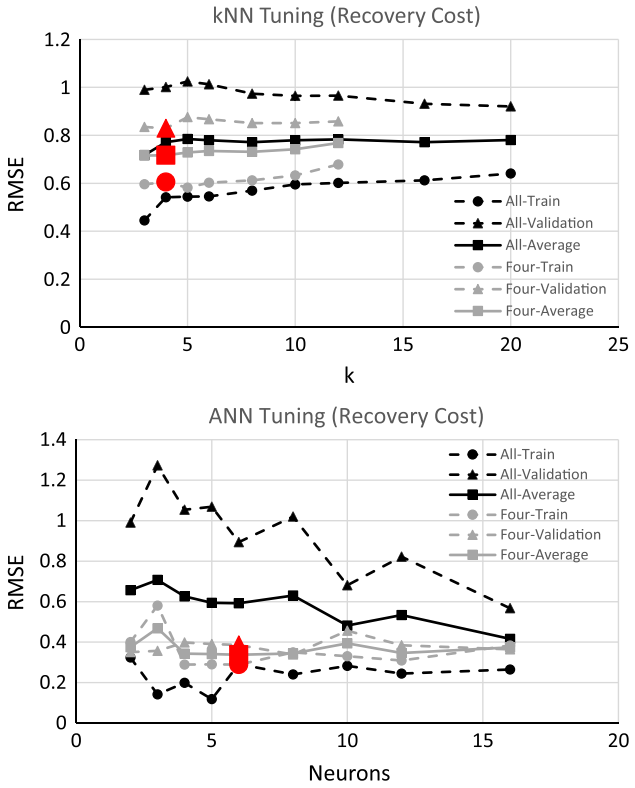

Fig. 10. Tuning of k-nearest neighbor and artificial neural network for recovery cost.

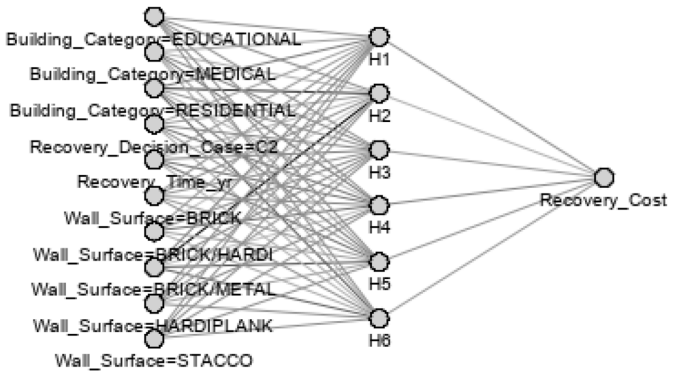

Fig. 11. ANN architecture for recovery cost.

Table 15. Comparison of RMSEs between regression and machine learning models for recovery cost

Model	Train data	Validation data	Model bias	Model variation
Linear regression	0.4224	0.5203	0.4713	0.0979
kNN $k = 4$	0.6045	0.829	0.717	0.2245
ANN $n = 6$	0.289	0.3861	0.338	0.0971
Gradient boosting $i = 200$	0.4118	0.4953	0.4535	0.0835

The kNN model with $k = 4$ and four significant input variables (building category, recovery decision, recovery time, and wall surface), the ANN model with 6 hidden layer neurons and the four significant input variables (as shown in Fig. 11), and the gradient boosting model with iteration = 200 were selected in the resilience analyses.

The comparison of RMSEs between the results of regression and machine learning models for recovery cost as the target variable is listed in Table 15. The comparison results showed that all models' biases are acceptable (0.34–0.48), except for the kNN model. The gradient boosting and ANN models had better prediction accuracy compared to other models.

Conclusions and Limitations

In this study, the relationship between the target resilience variables (recovery decision, recovery time, and recovery cost), and the nine input predictor variables (building category, building structure, wall surface material, roof surface material, building stories, blocked or not, distance from the blast center, year built, and shockwave overpressure) was established. The following conclusions were drawn:

- For the target variable of the *damage scale*, shockwave overpressure, distance, and blocked were the significant input variables. The logistic regression in Eqs. (8)–(10) could be used for simple applications of future prediction, which depict that the higher the blast load, the higher probability of the higher damage scale is expected. The logistic regression and all the machine learning models (kNN, ANN, and gradient boosting) can provide good predictive performance with acceptable accuracy. The model bias (average misclassification rate) in this case study was in the range of 0.07–0.08. The gradient boosting model performed better than others, which has the lowest model bias. However, the model varied more than the regression and ANN models.
- For the target variable of *recovery decision* (reconstruction or repair), shockwave overpressure, distance, damage level, and wall surface were the significant input variables. The logistic regression of Eqs. (11) and (12) could be used for simple applications of future prediction. When buildings were closer to the blast center and/or the blast load was higher, the probability of reconstruction was higher than the repair. The logistic regression and all the machine learning models (kNN, SVM, ANN, and gradient boosting) can provide good predictive models with acceptable accuracy. The model bias (average misclassification rate) in this case study was in the range of 0.04–0.11. The ANN and gradient boosting models provided better prediction accuracy compared to other models. However, the gradient boosting model varied more than the ANN model.
- For the target variable of *recovery time*, shockwave overpressure, damage level, and blocked were the significant input variables. The linear regression of Eq. (13) was proposed for simple applications of prediction, which showed that the damage scale negatively affected recovery time, indicating that a higher damage scale could result in a sooner rebuild or repair, the higher overpressure made for a longer recovery time, and the block protection for buildings can lower the recovery time. The linear regression and all the machine learning models (kNN, ANN, and gradient boosting) can provide good predictive models with acceptable accuracy. The model bias (average RMSE) in this case study was in the range of 0.75–1.20 years. The gradient boosting model can provide better prediction accuracy compared to other models. However, the gradient boosting model varied more than other models.
- For the target variable of *recovery cost*, building category, recovery decision, recovery time, and wall surface were the significant input variables. The linear regression in Eq. (15) was proposed for simple applications of prediction, which showed that (1) the building category affected recovery cost, indicating that the medical buildings needed the highest recovery costs,

educational buildings needed medium costs, and residential buildings needed the lowest costs; (2) the recovery decision affected recovery cost, in which reconstruction needed higher costs than repair; (3) recovery time positively affected recovery cost; and (4) wall surface material affected recovery cost, in which the cost was ranked from high to low in the following order: brick walls with hardiplank > hardiplank walls > brick walls > stucco > brick walls with metal plates. The linear regression and all the machine learning models (kNN, ANN, and gradient boosting) can provide good predictive models with acceptable accuracy. The model bias (average RMSE) in this case study was in the range of 0.34–0.48. The gradient boosting and ANN model can better predict accuracy compared to other models.

- Overall, for all target variables, the gradient boosting model outperformed all other models. However, it varied more among different data samples.

The results of this study can be used to assist government decision-makers, architects, civil engineers, and building designers in selecting the most resilient structure design and/or materials for a residential or commercial building and planning the most resilient buildings, communities, and cities by considering the impact of blast hazards. For example, Chi-square test results and ML models showed that the input variable of *blocked* significantly influences the target variable of damage scale and recovery time. Furthermore, the target variable of recovery cost is indirectly affected by blocked because recovery cost is significantly affected by recovery time, while recovery time is significantly affected by the variable of blocked. In this case study, blocked means the building was blocked from the explosion by trees, other buildings, and so forth. The Chi-square test and ML models indicated that the blocked significantly reduced damage scale, recovery time, and recovery cost. Gorev and Medvedev (2017) proposed that a screen be placed in its explosion wave path to protect houses from explosions. The experiments provided grounds to conclude that such obstacles can serve as effective explosion protection. The results of this study verified the idea of using protection screens to protect buildings from explosion damages and improve their resilience.

However, because the machine learning models created in this study were based on a single explosion case, there exist many limitations for applying the results of this study. For example, (1) the West explosion was caused by an ammonium nitrate (AN) explosion, so it may not be applicable for other explosion cases; (2) the West site condition had a flat ground surface, so the slope ground surface case may not be applicable; and (3) only 76 observations were documented and used for the ML modeling, so the data size is relatively small. The parameters obtained in this study may be sensitive to different cases. Therefore, the authors recommend that users adopt the proposed ML framework to create their own models instead of using the proposed equations/coefficients directly. The ML framework of this study could be adjusted and used for natural hazard resilience analysis as well.

Data Availability Statement

Some or all data, models, or codes that support the findings of this study are available from the corresponding author upon reasonable request.

References

Ahmadi, H., A. Yeganeh, A. H. Mohammadi, and E. Zavvar. 2016. "Probabilistic analysis of stress concentration factors in tubular KT-joints reinforced with internal ring stiffeners under in-plane bending loads." *Thin-Walled Struct.* 99 (1): 58–75. https://doi.org/10.1016/j.tws.2015.11.010.

Austin, P. C., and J. V. Tu. 2004. "Automated variable selection methods for logistic regression produced unstable models for predicting acute myocardial." *J. Clin. Epidemiol.* 57 (11): 1138–1146. https://doi.org/10.1016/j.jclinepi.2004.04.003.

Babrauskas, V. 2016. "Explosions of ammonium nitrate fertilizer in storage or transportation are preventable accidents." *J. Hazard. Mater.* 304 (Mar): 134–149. https://doi.org/10.1016/j.jhazmat.2015.10.040.

Babrauskas, V. 2017. "The West, Texas, ammonium nitrate explosion: A failure of regulation." *J. Fire Sci.* 35 (5): 396–414. https://doi.org/10.1177/0734904116685723.

Bergstrand, K., B. Mayer, B. Brumback, and Y. Yi Zhang. 2015. "Assessing the relationship between social vulnerability and community resilience to hazards." *Soc. Indic. Res.* 122 (2): 391–409. https://doi.org/10.1007/s11205-014-0698-3.

Capozzo, M., A. Rizzi, G. P. Cimellaro, M. Domaneschi, A. Barbosa, and D. Cox. 2019. "Multi-hazard resilience assessment of a coastal community due to offshore earthquake." *J. Earthquake Tsunami* 13 (2):1950008: https://doi.org/10.1142/S1793431119500088.

Chai, T., and R. R. Draxler. 2014. "Root mean square error (RMSE) or mean absolute error (MAE)? -Arguments against avoiding RMSE in the literature." *Geosci. Model Dev.* 7 (Jan): 1247–1250. https://doi.org/10.5194/gmd-7-1247-2014.

Davis, S., T. DeBold, and C. Marsegan. 2017. "Investigation findings and lessons learned in the west fertilizer explosion." *J. Fire Sci.* 35 (5): 379–395. https://doi.org/10.1177/0734904117715649.

Dhulipala, S. L. N., and M. M. Flint. 2020. "Series of semi-Markov processes to model infrastructure resilience under multi-hazards." *Reliab. Eng. Syst. Saf.* 193 (Mar): 106659. https://doi.org/10.1016/j.ress.2019.106659.

Egnew, A. C., D. B. Roueche, and D. O. Prevatt. 2018. "Linking building attributes and tornado vulnerability using a logistic regression model." *Nat. Hazards Rev.* 19 (4): 4018017. https://doi.org/10.1061/(ASCE)NH.1527-6996.0000305.

Eskew, E. L., and S. Jang. 2020. "Remaining capacity estimation for buildings after an explosion using the adaptive alternate path analysis." *Adv. Struct. Eng.* 23 (4): 630–641. https://doi.org/10.1177/1369433219876212.

FEMA. 2011. *Hazards U.S. multi-hazard (HAZUS MH) assessment tool*. Washington, DC: FEMA.

Gorev, V., and G. Medvedev. 2017. "The flexible perforated screens are a protection of buildings against external explosions." In *Proc., Int. Science Conf. SPbWOSCE-2016 "SMART City"*. Les Ulis, France: EDP Sciences. https://doi.org/10.1051/matecconf/201710602028.

Gujar, R., and V. Vakharia. 2019. "Prediction and validation of alternative fillers used in micro-surfacing mix-design using machine learning techniques." *Constr. Build. Mater.* 207 (2): 519–527. https://doi.org/10.1016/j.conbuildmat.2019.02.136.

Han, Z., H. J. Pasman, and M. S. Mannan. 2017. "Extinguishing fires involving ammonium nitrate stock with water: Possible complications." *J. Fire Sci.* 35 (6): 457–483. https://doi.org/10.1177/0734904117735264.

Han, Z., S. Sachdeva, M. I. Papadaki, and S. Mannan. 2016. "Effects of inhibitor and promoter mixtures on ammonium nitrate fertilizer explosion hazards." *Therm. Acta* 624 (1): 69–75. https://doi.org/10.1016/j.tca.2015.12.005.

Huang, Z., K. Dai, J. Wang, and H. F. Wu. 2016. "Investigations of structural damage caused by the fertilizer plant explosion at West, Texas. I: Air-blast incident overpressure." *J. Perform. Constr. Facil.* 30 (4): 04015064. https://doi.org/10.1061/(ASCE)CF.1943-5509.0000799.

Huang, Z., X. Wang, L. Cai, Y. Tao, W. J. Tolone, M. El-Shambakey, S. D. Bhattacharjee, and I. Isaac Cho. 2020. "Blast risk assessment of wood residential buildings: West fertilizer plant explosion case." *J. Perform. Constr. Facil.* 34 (3): 04020022. https://doi.org/10.1061/(ASCE)CF.1943-5509.0001414.

Jennings, K., and C. Matthiessen. 2015. "Update: EPA actions—Chemical safety and security executive order." *Process Saf. Prog.* 34 (2): 196–198. https://doi.org/10.1002/prs.11707.

Jonkeren, O., and G. Giannopoulos. 2014. "Analysing critical infrastructure failure with a resilience inoperability input-output model." *Econ. Syst. Res.* 26 (3): 39–59. https://doi.org/10.1080/09535314.2013.872604.

Kumar, M., N. S. Raghuwanshi, and R. Singh. 2011. "Artificial neural networks approach in evapotranspiration modeling: A review." *Irrig. Sci.* 29 (1): 11–25. https://doi.org/10.1007/s00271-010-0230-8.

Kumaraswamy, M., W. Zou, and J. Zhang. 2015. "Reinforcing relationships for resilience-by embedding end-user 'people' in public-private partnerships." *Civ. Eng. Environ. Syst.* 32 (2): 119–129. https://doi.org/10.1080/10286608.2015.1022727.

Laboureur, D. M., et al. 2016. "Case study and lessons learned from the ammonium nitrate explosion at the West Fertilizer facility." *J. Hazard. Mater.* 308 (May): 164–172. https://doi.org/10.1016/j.jhazmat.2016.01.039.

Li, Q., J. Zhang, and H. Jiang. 2019. "Incorporating multi-source remote sensing in the detection of earthquake-damaged buildings based on logistic regression." *Nat. Hazards Earth Syst. Sci. Discuss.* 2019 (May): 1–26. https://doi.org/10.5194/nhess-2019-20.

Liu, Y., J. Wei, J. Xu, and Z. Ouyang. 2018. "Evaluation of the moderate earthquake resilience of counties in China based on a three-stage DEA model." *Nat. Hazards* 91 (2): 587–609. https://doi.org/10.1007/s11069-017-3142-6.

Masoomi, H., M. R. Ameri, and J. W. van de Lindt. 2018. "Wind performance enhancement strategies for residential wood-frame buildings." *J. Perform. Constr. Facil.* 32 (3): 04018024. https://doi.org/10.1061/(ASCE)cf.1943-5509.0001172.

Melgani, F., and L. Bruzzone. 2004. "Classification of hyperspectral remote sensing images with support vector machines." *IEEE Trans. Geosci. Remote Sens.* 42 (8): 1778–1790. https://doi.org/10.1109/TGRS.2004.831865.

Modica, M., and R. Zoboli. 2016. "Vulnerability, resilience, hazard, risk, damage, and loss: A socio-ecological framework for natural disaster analysis." *Web Ecol.* 16 (1): 59–62. https://doi.org/10.5194/we-16-59-2016.

Noi, P. T., and M. Kappas. 2018 "Comparison of random forest, k-nearest neighbor, and support vector machine classifiers for land cover classification using Sentinel-2 imagery." *Sensors* 18 (1): 18. https://doi.org/10.3390/s18010018.

Opdyke, A., A. Javernick-Will, and M. Koschmann. 2017. "Infrastructure hazard resilience trends: An analysis of 25 years of research, natural hazards (Dordrecht)." 87 (2): 773–789. https://doi.org/10.1007/s11069-017-2792-8.

Parzen, M., S. Ghosh, S. Lipsitz, D. Sinha, G. M. Fitzmaurice, B. K. Mallick, and J. G. Ibrahim. 2011. "A generalized linear mixed model for longitudinal binary data with a marginal logit link function." *Ann. Appl. Stat.* 5 (1): 449–467. https://doi.org/10.1214/10-AOAS390.

Reuters. 2013. "Ammonium nitrate was trigger for Texas blast, state agency says." Accessed September 7, 2020. https://www.reuters.com/article/us-usa-explosion-texas/ammonium-nitrate-stores-exploded-at-texas-plant-state-agency-idUSBRE9460GP20130507.

Russo, P., A. De Marco, and F. Parisi. 2019. "Failure of reinforced concrete and tuff stone masonry buildings as consequence of hydrogen pipeline explosions." *Int. J. Hydrogen Energy* 44 (38): 21067–21079. https://doi.org/10.1016/j.ijhydene.2019.01.225.

Song, B., W. Jiao, K. Cen, X. Tian, H. Zhang, and W. Lu. 2021. "Quantitative risk assessment of gas leakage and explosion accident consequences inside residential buildings." *Eng. Fail. Anal.* 122 (23): 105257. https://doi.org/10.1016/j.engfailanal.2021.105257.

Tso, G. K. F., and K. K. W. Yau. 2007. "Predicting electricity energy consumption: A comparison of regression analysis, decision tree, and neural networks." *Energy* 32 (9): 1761–1768. https://doi.org/10.1016/j.energy.2006.11.010.

USBDC (United States Bomb Data Center). 2019. "The annual explosives incident report (EIR)." Accessed February 18, 2021. file:///C:/Users/Lenovo/Dropbox/Zhenhua%20Huang/Temp/2019_explosives_incident_report_0.pdf.

Yonekawa, Y., et al. 2014. "Ocular blast injuries in mass-casualty incidents the marathon bombing in Boston, Massachusetts, and the fertilizer plant explosion in West, Texas." *Ophthalmology* 121 (9): 1670–1676. https://doi.org/10.1016/j.ophtha.2014.04.004.

Yuan, S. 2015. "Random gradient boosting for predicting conditional quantiles." *J. Stat. Comput. Simul.* 85 (18): 3716–3726. https://doi.org/10.1080/00949655.2014.1002099.